

# Blackout mitigation in a plasma layer near a high-speed body in ExB fields

S A Poniaev<sup>1,3</sup>, Y A Kurakin<sup>1</sup>, A A Schmidt<sup>1</sup>, S V Bobashev<sup>1</sup>, L Steffens<sup>2</sup>,  
B Esser<sup>2</sup>, A Gulhan<sup>2</sup>

<sup>1</sup>Ioffe Physico-technical Institute, St. Petersburg, Russia

<sup>2</sup>Institute of Aerodynamics and Flow Technology, DLR, Cologne, Germany

E-mail: serguei.poniaev@mail.ioffe.ru

**Abstract.** The space vehicle deceleration at reentry into the atmosphere leads to aerodynamic heating and, hence, ionization of near-wall plasma layers. The plasma layer causes radio communication blackout. This report discusses the possibility to provide a blackout mitigation by changing the plasma parameters near the body with the help of the magnetohydrodynamic (MHD) effects. The numerical simulations were carried out for the conditions corresponding to those at the DLR test facility.

## 1. Introduction

During interplanetary missions or re-entry flights to the earth the communication between the spacecraft and control station on the earth may interrupt. In the frame of the project ‘ „Communication Blackout Migration for Spacecraft – COMBIT“ the scientists of two Helmholtz Centers – German Aerospace Center (DLR) in Cologne and Karlsruhe Institute of Technology (KIT) – develop in co-operation with the scientists of the IOFFE Physical-Technical Institute of the Russian Academy of Sciences in Saint-Petersburg a new method to solve this problem.

When a vehicle enters the radio blackout phase, it loses all communication including GPS signals, data telemetry, and voice communication. Blackout occurs when the radio waves used for communication between ground stations and satellites are attenuated and/or reflected by the plasma layer that is created during hypersonic/re-entry flight. This phenomenon was well known at the beginning of space exploration when space capsule would experience several minutes of radio blackout during re-entry. Nearly 50 years later, hypersonic capsules still experience radio blackout during re-entry.

Maximum heating at the reentry trajectories of reusable space vehicles occurs at the heights ranging from 80 to 60 km, the temperature in the near-wall layers can reach in this case  $10^4$  K. In this situation the electron density can reach  $n_e \approx 10^{17} - 10^{20} \text{ m}^{-3}$ , and the characteristic plasma frequency in the near-wall layer of the ionized gas which is equal to  $f_p = 0.9 \times 10^4 \sqrt{n_e}$  is in the range 2.85 – 90 GHz [1-3]. This causes reflection and attenuation of radio signals the frequencies of which are lower than the plasma frequency, and the plasma layer near the vehicle plays the role of a screen that blocks transmission of electromagnetic waves with the frequencies used for communication with space

<sup>3</sup> Author to whom any correspondence should be addressed.



vehicles (the so-called communication blackout occurs). The time of blackout at the stage of vehicle reentry into the atmosphere can be as long as 20 min.

The COMBIT team tries to solve the radio blackout problem by reducing the electron number density of the plasma layer. This should be achieved by means of magneto-hydrodynamic (MHD) effects [4,5]. A combined magnetic and electrical field created close to the antenna should deflect charged particles in such a way that a local gas layer with low plasma frequency forms and the communication between the control station and spacecraft is guaranteed.

## 2. Planned experiments

DLR is responsible for the design and conducting experiments in the arc heated facility L2K, which allows producing ionized hypersonic flow with a total temperature of several thousand degrees. At such temperatures the gas is composed of molecules, atoms, ions and electrons.

In L2K [6,7] the ionized high temperature gas is test model is accelerated to hypersonic speeds using a supersonic nozzle. Fig.1 shows a schematic of L2K facility. Inside the extension part of nozzle and in the free stream the velocity but the temperature, pressure and density decrease. But in front of the model a bow shock forms and decelerates the flow. The shock heats the gas to temperatures, at which the flow is ionized. The magnet is mounted in the middle part of the model. Two electrodes for producing electrical field are integrated on the model surface upstream and downstream of the magnet. The sending antenna inside the model is placed close to the downstream electrode. Its signal has to pass the ionized flow before reaching the receiving antenna, which is placed outside the flow.

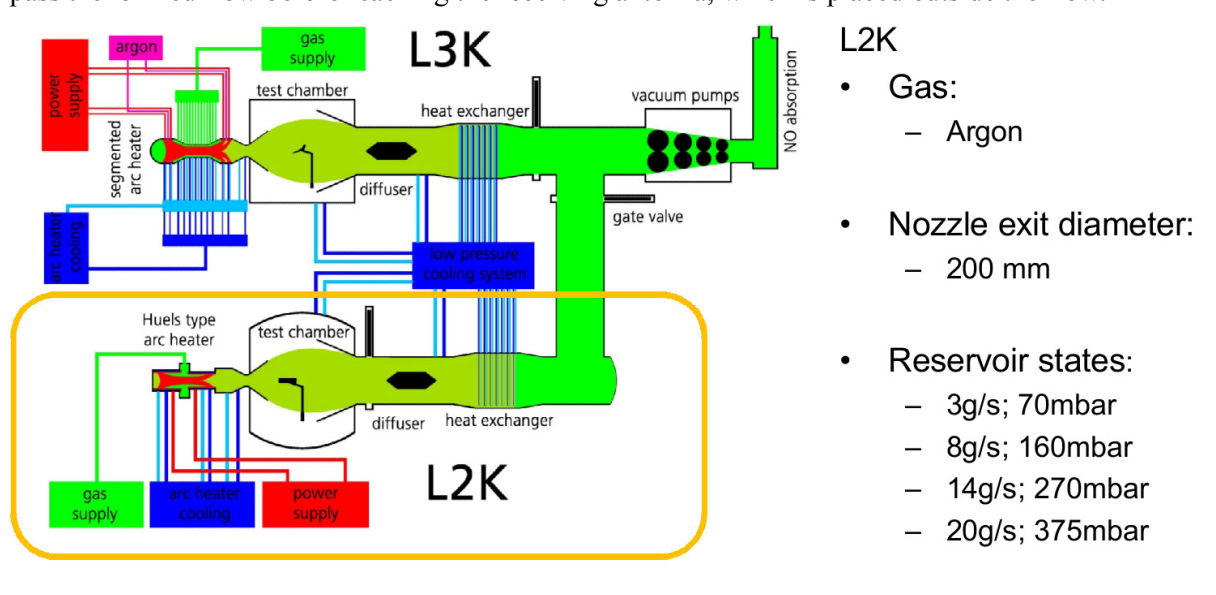


**Figure 1.** Schematic of L2K facility at DLR, Cologne

In L2K the ionization of the flow is weaker compared to the flight conditions with black-out effects. Therefore the experiments have to be carried out at higher intensity of the magnetic field, which cannot be realized with permanent magnets. Only cooled superconductive magnets are able to achieve magnetic field intensities beyond 2 Tesla on the model surface. The compact size superconducting magnet of KIT is cooled down to 4 Kelvin, i.e. -269°Celsius using Helium as coolant. Another very challenging requirement is the sufficient and reliable thermal isolation of the magnet from the high temperature environment of the flow.

During preliminary tests it could be demonstrated that even in the weakly ionized flow of L2K the attenuation of the communication signal can be measured clearly. These tests showed also some positive effect of the permanent magnets with a magnetic field strength of 1 Tesla are measurable. The main tests with superconducting magnets are planned in end of 2014.

### 3. Numerical simulation

The goal of our study was to estimate whether it is possible to affect the flow structure by the MHD methods with the aim of achieving a local decrease in the electron concentration near the antenna. To this end, by using external magnetic and electric fields produced by a coil placed in the body and a system of electrodes situated at its surface (see Fig. 2), a region of electromagnetic interaction between the plasma flow and external  $\vec{E} \times \vec{B}$  fields is generated. Two fundamentally different electrode orientations are considered: 1) electrodes are orientated perpendicularly to the incoming flow (Fig. 2 (a)), 2) electrodes are parallel to the incoming flow (Fig. 2 (b)).

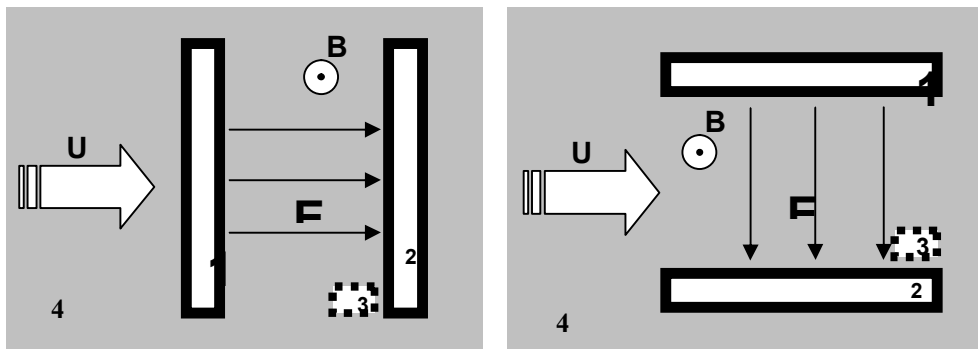


**Figure 2.** Scheme of electrodes on the model surface and magnetic field for creation of «magnetic window»: (a) – electrodes (1 is anode and 2 is cathode) are perpendicular to the flow; (b) – electrodes (1 and 2) parallel to the incoming flow; 3 is possible antenna position, 4 – surface of model.

To carry out the estimates, the model of a three-component plasma consisting of atoms, ions, and electrons was used. A stationary flow along the plane simulating the space vehicle surface is considered. The model is based on the following assumptions: 1) the neutral component moves with a constant uniform velocity; 2) the gradient of electron pressure in the plasma layer of interest can be neglected; 3) the plasma layer has a small thickness, all MHD processes occur inside this layer, the electric field in the immediate vicinity of the electrodes is uniformly distributed throughout the layer thickness, there is no electric field across the layer, and all plasma parameters are constant across the layer; 4) the magnetic induction vector is directed perpendicularly to the space vehicle surface across the plasma layer.

Thus the problem of the motion of charged particles is reduced to the solution of Ohm's law which allows one to obtain distributions of the potential and total current. The distribution of the ion concentration is obtained by using the continuity equation for ions.

If we use these assumptions and take into account the ion slip and Hall effect, the equation for the generalized Ohm's law is

$$\vec{j} = \sigma \frac{(1+s) \left( \vec{E} + \vec{U} \times \vec{B} + \frac{\nabla p_e}{en_e} \right) - \beta_e \left( \vec{E} + \vec{U} \times \vec{B} + \frac{\nabla p_e}{en_e} \right) \times \vec{b}}{(1+s)^2 + \beta_e^2}$$

where  $u \approx (n_i u_i + n_a u_a) / (n_i + n_a)$ ,  $U_k = u_k - u$ ,  $\vec{b} = \vec{B} / B$ , indexes  $e, i, a$  refer to electrons, ions and atoms, respectively,  $\sigma, s, \beta_e$  are the coefficient of electric conductivity of electrons, coefficient

of ion slip and Hall parameter for electrons, respectively. For the flow under consideration these parameters can be estimated as  $\beta_e \approx 600 \cdot B \gg 1$ ,  $s \approx 200 \cdot B \gg 1$ .

If we take into account that in our case  $t_0 \gg \nu_{ia}^{-1}$  and  $m_e v_{ie} \ll m_a v_{ia}$  and also that  $u \approx u_a$  at a low ionization degree, and  $U_a \approx 0$ , and also that  $n_e k T_a \ll n_e m_a v_{ia} u_0$ , we obtain the expression for the ion velocity

$$U_i = \frac{\sigma_{i\perp} E' + \sigma_{iH} (b \times E')}{en_e},$$

where  $\vec{E}' = \vec{E} + \vec{U} \times \vec{B}$ ,  $\sigma_i$  is the coefficient of electric conductivity of ions,  $\nu_{kl}$  is the collision frequency of particles of  $k$  and  $l$  classes, and  $m_l$  is the mass of  $l$  class particle. Therefore, we can find the ion velocity  $u_i = u + U_i$ . The distribution of ion concentrations can be determined by solving the continuity equation

$$\nabla(n_i u_i) = 0.$$

The ion concentration at the inlet boundary of the computational domain was taken to be  $n_i = 2.81 \cdot 10^{17} \text{ m}^{-3}$ , the velocity of the incoming flow was 2250 m/s. The computational domain size considerably exceeded the characteristic size of the interelectrode gap in order to fulfill the condition  $U_i \approx 0$  at the boundaries.

Fig 3 shows distribution of ion concentration for three cases: (i) the direction of the plasma flow coincides with direction of the applied electric field (potential difference is 100 V) (Fig.3(a)); (ii) the direction of the applied electric field (potential difference is 100 V) is opposite to the direction of the plasma flow (Fig.3(b)) and (iii) direction of the applied electric field is perpendicular to the direction of the plasma flow (potential difference is 900 V) (Fig.3(c)). Because of the absence of charge separation in the flow the distributions of ion concentration is equal to the distribution of electron concentration, which is responsible for the effects of communication blackout.

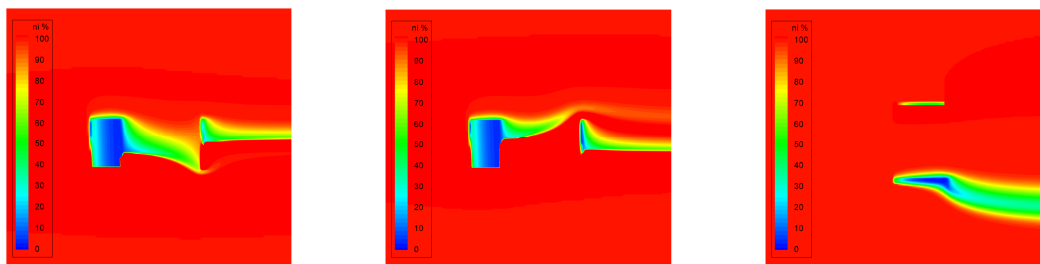


**Figure 3.** Distribution of normalized ion concentration near the model surface: (a) – are perpendicular to the flow; (b) – electrodes are perpendicular to the flow, electric field have the other direction than is case (a); (c) – electrodes are parallel to the flow.

It can be seen that in the first two cases a noticeable decrease in the ion concentration is observed immediately after the first electrode irrespective of whether it is anode or cathode. The applied field direction plays a minor role because the intensity of the electric field that arises in the plasma moving in the magnetic field is much higher than that of the applied field. In the configuration where electrodes are normal to the flow the plasma flow is decelerated, and the applied electric field direction affects only the size and direction of the zone of a reduced ion concentration. In the case when electrodes are parallel to the incoming plasma flow, the electromagnetic interaction causes

acceleration of the plasma flow. The zone of reduced ion concentration is near the cathode, it extends down the flow near the outer side of the cathode.

These results allow us to formulate preliminary recommendations on formation of the external field configuration for affecting plasma flow parameters.

In particular, when electrodes are parallel to the plasma flow and the MHD interaction provides its acceleration, the most suitable place for the antenna can be out of the interelectrode gap.

### **Acknowledgements**

The work was supported by RFBR grant 12-01-91320-SIG\_a.

### **References**

- [1] Boyd I D, 2007, AIAA 2007-206
- [2] Hartunian R A, Stewart G E, Ferguson S D, Curtiss T J, and Seibold R W, 2007 Aerospace report ATR 2007(5309)-1
- [3] Lehnert R, Rosenbazlm B, 1965 NASA TN D-2732
- [4] Kim M, Keidar M, Boyd I B 2009 AIAA 2009-1232
- [5] Kim M, Boyd I D, Keidar M, Jones C H, Beilis I, Pekker L, Raitses Y, Levchenko I, 2010, Journal of Spacecraft and Rockets vol 47 p 29
- [6] Gülhan A, Esser B, and Koch U, 2001 Journal of Spacecraft and Rockets vol. 38 no 2 p 199
- [7] Gülhan A, and Esser B, 2002 Advanced Hypersonic Test Facilities, Progress in Astronautics and Aeronautics vol 198 pp 375-403